



Laminar Instability of Parallel and Nonparallel Flows of Adiabatic Flat Plate

Y. Mérida[†], M. Jelliti and T. Lili

Laboratory of Fluid Mechanics (LMF), Faculty of Sciences of Tunis (FST), University El Manar (UM), University Campus, 2092 El Manar II, Tunis, Tunisia

[†]Corresponding Author Email merida_yo@yahoo.fr

(Received March 13, 2016; accepted November 19, 2016)

ABSTRACT

In the present paper, spatial linear stability of adiabatic laminar flat plate boundary layer is computed numerically. This work is interested on the non-parallel compressible flow for a two-dimensional (2D) and three-dimensional (3D) disturbances. Stability diagrams, in the form of curves of constant spatial amplification rates are presented and constitute the original contribution of this paper. However, to assess the validity of the present computations, some important results of parallel flow stability are presented in the convenient and familiar form of contours of constant spatial amplification rates for both 2D and 3D waves in the Mach number range $Me=0.9$ to 2.2 . Comparisons results for the parallel flow agree with those obtained by Mack and Wazzan, Taghavi and Keltner, but differ from the nonparallel flow giving some important spatial stability results and showing the importance of the wave angle ψ and the Mach number, even the stability diagrams presented in this paper concerned the Reynolds number gives different results for the parallel and nonparallel flows.

Keywords: Laminar instability; Compressible boundary layer; Transonic flow; Supersonic flow; Stability diagrams.

1. INTRODUCTION

Laminar flow has been the object of study by several generations of investigators. One of the earliest explanations was that laminar flow is unstable, and the linear instability theory was first developed to explore this possibility. The most important theoretical investigation to date of the stability of the compressible boundary layer was carried out by Lees and Lin (1946). They developed an asymptotic theory in close analogy to the incompressible asymptotic theory of Lin (1945). A numerical method of solving the Lees-Lin, and the Dunn-Lin equations (1947), were first given by Brown (1961, 1962). Later, Mack presented another numerical method for solving the stability equations for the compressible laminar flat plate boundary layer (1965a, 1965b). A comprehensive investigation on general computational using parallel performance identifies the numerical methods for the linear stability (1990, 2004, and 2008).

Because of the failure of the parallel theories to predict the critical Reynolds number for the Blasius flow, considerable interest has developed in nonparallel stability analysis. Some incomplete attempts to account for nonparallel flow effects involved the retention of the normal component of the velocity or some of the streamwise derivatives of

the primary flow. Others used different expansion techniques and different conditions for separating variables. A summary of these papers was given by Saric and Nayfeh (1975). A number of works concerned with the nonparallel linear stability analyses using different methods and applications have been published (1993, 1997, and 2007).

In the present paper, we compute numerically the effect of Mach number on the spatial linear stability of adiabatic laminar flat plate boundary layer, applied to the parallel flow, in the Mach number range 0.9 to 2.2 and the non-parallel flow for 2D and oblique disturbances in the range Mach number 0.9 and 1.1 . Numerical methods using for solving the stability equations are given in details in section 2. Comparison results made in section 3 give similarity and differences between the parallel and non-parallel flows.

2. STABILITY EQUATIONS AND NUMERICAL PROCEDURE

We start in this first section by recalling the general equations governing the flow of a compressible viscous fluid with the properties of perfect gas fluid, Sutherland's law of viscosity, constant Prandtl number and constant specific heat C_v (at constant volume).

2.1. General Equations in Intrinsic Tensoriel Notation

The equations are, respectively, of continuity, momentum, energy and state with $u_i = (u, v, w)$ are the velocities in the (x,y,z) directions, respectively, where x is the streamwise and z the spanwise coordinate; p is the pressure, ρ is the density, R is the gas constant, T is the temperature, μ , λ are the viscosity coefficients, C_v is the specific heat at constant volume and λ_c is the thermal conductivity.

Continuity Equation:

$$\frac{\partial \rho}{\partial t} + \text{div}(\rho \bar{v}) = 0 \quad (1)$$

Momentum Equation:

$$\frac{\partial \bar{v}}{\partial t} + \text{grad} \bar{v} \cdot \bar{v} = \frac{1}{\rho} \text{div} \Sigma \quad (2)$$

Where Σ is the stress tensor,

$$\Sigma = [(-p + \text{div} \bar{v})I + 2\mu D] \quad (3)$$

(I is the identity tensor) and D is the strain rate tensor

$$D = \frac{1}{2} [\text{grad} \bar{v} + \text{grad} \bar{v}] \quad (4)$$

Energy Equation:

$$\frac{\partial e}{\partial t} + \text{grad} e \cdot \bar{v} = \frac{1}{\rho} \Sigma : D + \frac{1}{\rho} \text{div}(\lambda_c \text{grad} T) \quad (5)$$

The gas considered is a perfect gas and the internal energy e is function of temperature:

$$de = C_v(T) dT \quad (6)$$

An equivalent form of energy equation is:

$$\rho \frac{\partial e}{\partial t} + \rho \text{grad} e \cdot \bar{v} = \Sigma : D + \lambda_c \Delta T + \text{grad} T \cdot \text{grad} \lambda_c \quad (7)$$

Where $\Sigma : D$ is the double contraction between the tensor Σ and D.

We adopt in this paper another equivalent form of energy equation:

$$C_v \left[\rho \frac{\partial T}{\partial t} + \rho \text{grad} T \cdot \bar{v} \right] = -p \text{div} \bar{v} + \lambda (\text{div} \bar{v})^2 + 2\mu D : D + \lambda_c \Delta T + \text{grad} T \cdot \text{grad} \lambda_c \quad (8)$$

$$\text{Equation of state: } p = \rho RT \quad (9)$$

2.2. General Equations in Index Notations

We adopt index notations for clarity, where the Einstein summation rule applies to repeated indices

Continuity Equation:

$$\frac{\partial \rho}{\partial t} + (\rho u_i)_i = 0 \quad (10)$$

Momentum Equation:

$$\rho \frac{\partial u_i}{\partial t} + \rho u_{i,j} u_j = -p_{,i} + (\lambda + \mu) u_{i,jj} + \mu u_{i,jj} + u_{j,i} \lambda_{,i} + (u_{i,j} + u_{j,i}) \mu_{,j} \quad (11)$$

Energy Equation:

$$C_v \left[\rho \frac{\partial T}{\partial t} + \rho u_j T_{,j} \right] = -\rho u_{j,j} + \lambda u_{j,j} u_{k,k} + 2\mu D_{ij} D_{ij} + \lambda_c T_{,ij} + T_{,j} \lambda_{c,j} \quad (12)$$

$$\text{Equation of state: } p = \rho RT \quad (13)$$

2.3. Mean Flow and Perturbations Equations

All quantities are divided into a steady mean-flow (denoted by an overbar) and an unsteady small disturbance term (denoted by a prime)

Formulation:

$$u = \bar{u} + u', v = \bar{v} + v', w = \bar{w} + w', \rho = \bar{\rho} + \rho', p = \bar{p} + p' \\ T = \bar{T} + T', \mu = \bar{\mu} + \mu', \lambda = \bar{\lambda} + \lambda', \lambda_c = \bar{\lambda}_c + \lambda'_c \quad (14)$$

We retain up to now, the hypothesis that the mean values $(\bar{u}, \bar{v}, \bar{w}, \bar{\rho}, \bar{p}, \bar{T})$ are functions of one space variable, y. In this work, this hypothesis defines the non-parallel flow; if additional more used $\bar{v} = 0$ is imposed, the flow is conventionally called quasi-parallel flow. In the application which is contemplated and which involves the study of the stability of a three dimensional boundary layer of compressible flow over a flat plate, the y coordinate is along the normal to the plate.

$$\bar{u}_i = (\bar{u}(y), \bar{v}(y), \bar{w}(y)), \bar{\rho} = \bar{\rho}(y), \bar{p} = \bar{p}(y), \\ \bar{T} = \bar{T}(y), \bar{\mu} = \bar{\mu}(T), \bar{\lambda} = \bar{\lambda}(T), \bar{\lambda}_c = \bar{\lambda}_c(T) \quad (15)$$

The transport coefficients are functions only of temperature, so that their fluctuations can be written in first order approximation:

$$\mu' = \frac{d\bar{\mu}}{dT} T', \lambda' = \frac{d\bar{\lambda}}{dT} T', \lambda'_c = \frac{d\bar{\lambda}_c}{dT} T' \quad (16)$$

However, we indicate the properties of the derivatives of $\bar{\mu}$ and μ' , respectively, this same properties hold for $\bar{\lambda}$, λ' and $\bar{\lambda}_c$, λ'_c

$$\frac{\partial \bar{\mu}}{\partial x} = \frac{\partial \bar{\mu}}{\partial z} = 0, \frac{\partial \bar{\mu}}{\partial y} = \frac{d\bar{\mu}}{dT} \frac{dT}{dy}, \frac{\partial \mu'}{\partial x} = \frac{d\bar{\mu}}{dT} \frac{dT'}{dx}, \frac{\partial \mu'}{\partial z} = \frac{d\bar{\mu}}{dT} \frac{dT'}{dz}, \\ \frac{\partial \mu'}{\partial y} = T' \frac{d^2 \bar{\mu}}{dT^2} \frac{dT}{dy} + \frac{d\bar{\mu}}{dT} \frac{dT'}{dy} \quad (17)$$

We should note that the mean flow and the resulting flow satisfy the equations of motion and the disturbance imposed on the mean flow is small such that the nonlinear terms can be neglected. Subsequently, we obtain the following equations:

Continuity Equations:

$$\frac{\partial}{\partial x}(\overline{\rho u}) + \frac{\partial}{\partial y}(\overline{\rho v}) + \frac{\partial}{\partial z}(\overline{\rho w}) = 0 \quad (18)$$

$$\begin{aligned} \frac{\partial \rho'}{\partial t} + \frac{\partial}{\partial x}(\overline{u\rho'} + \overline{\rho u'}) + \frac{\partial}{\partial y}(\overline{v\rho'} + \overline{\rho v'}) \\ + \frac{\partial}{\partial z}(\overline{w\rho'} + \overline{\rho w'}) = 0 \end{aligned} \quad (19)$$

Momentum Equations :

$$\overline{\rho u_{i,j} u_j} = -\overline{p_{,i}} + (\overline{\lambda} + \overline{\mu}) \overline{u_{j,ji}} + \overline{\mu u_{i,ji}} + \overline{u_{j,i} \lambda_{,i}} \quad (20)$$

$$\begin{aligned} \overline{\rho \frac{\partial u_i}{\partial t}} + \overline{\rho u_i u'_{i,j}} + \overline{\rho u_{i,j} u'_j} + \overline{\rho' u_{i,j} u_j} = -\overline{p'_{,i}} + (\overline{\lambda} + \overline{\mu}) \overline{u'_{j,ji}} \\ + \overline{u_{j,ji}} \left(\frac{d\overline{\mu}}{dT} + \frac{d\overline{\lambda}}{dT} \right) T' + \overline{\mu u'_{i,ji}} + \overline{u_{i,ji}} \frac{d\overline{\mu}}{dT} T' + \overline{u'_{j,i} \lambda_{,i}} \\ + \overline{u_{j,i} u'_{,i}} + (\overline{u'_{i,j}} + \overline{u'_{j,i}}) \overline{\mu_{,j}} + (\overline{u_{i,j}} + \overline{u_{j,i}}) \overline{\mu'_{,j}} \end{aligned} \quad (21)$$

Energy Equations:

$$\begin{aligned} C_v \left[\overline{\rho \frac{\partial T}{\partial t}} + \overline{\rho u_j T_{,j}} \right] = -\overline{p u_{j,j}} + \overline{\lambda u_{j,j} u_{k,k}} + 2\overline{\mu D_{ij} D_{ij}} \\ + \overline{\lambda_c T_{,jj}} + \overline{T_{,j} \lambda_{c,j}} \end{aligned} \quad (22)$$

$$\begin{aligned} C_v \left[\overline{\rho \frac{\partial T'}{\partial t}} + \overline{\rho T_{,j} u'_j} + \overline{\rho u_j T'_{,j}} + \overline{u_j T_{,j} \rho'} \right] = -\overline{p u'_{j,j}} \\ - \overline{u_{j,j} p'} + 2\overline{\lambda u_{k,k} u'_{j,j}} + \overline{\lambda' u_{j,j} u_{k,k}} + 4\overline{\mu D_{ij} D'_{ij}} \\ + 2\overline{\mu' D_{ij} D_{ij}} + \overline{\lambda_c T'_{,jj}} + \overline{T_{,jj} \lambda'_{c,j}} + \overline{T_{,j} \lambda'_{c,j}} + \overline{\lambda_{c,j} T'_{,j}} \end{aligned} \quad (23)$$

Equations of State:

$$\overline{p} = \overline{\rho r T} \quad (24)$$

$$p' = r(\overline{T} \rho' + \overline{\rho} T') \quad (25)$$

The boundary conditions at $y = 0$ are $u'(0) = v'(0) = w'(0) = T'(0) = 0$ (26)

The boundary conditions at $y \rightarrow \infty$ are: $u'(y), v'(y), w'(y), \rho'(y), p'(y), T'(y) \rightarrow 0$ or are bounded as $y \rightarrow \infty$ (27)

2.4. Stability Equations

Before proceeding to give nonparallel stability equations for the present formulation, it is noted that spatial amplification theory is considered in this work, where α and β (the x and z components of the wavenumber vector \vec{k}) are complex, ω (the frequency) is real, the amplitude will change with x, however, if α and β are real, and ω is complex, the amplitude will change with time, the former case is referred to as the temporal amplification theory. If all three quantities are complex, the disturbance will grow in space and time. The original, and for many years the only, form of the theory was the temporal theory. However, in a steady mean flow the amplitude of a normal mode is independent of time and changes only with distance. The spatial theory, which was introduced by Gaster (1965), gives this amplitude change in a more direct manner than does

the temporal theory.

For the special boundary layers to be considered in this paper, spatial wave is defined to be amplified or damped according to whether its amplitude increases or decreases in the x direction. Therefore, the three possible cases are: $-\alpha_i < 0$ damped wave, $-\alpha_i = 0$ neutral wave and $-\alpha_i > 0$ amplified wave.

The flow undisturbed being stationary and obviously the flow disturbance is not stationary. The system of equations describing the disturbed flow will have particular solutions of the form:

$$(u', v', w', p', \rho', T') = (f, \varphi, h, \pi, r, \theta) \exp[i(\alpha x + \beta z - \omega t)] \quad (28)$$

In the case where the unperturbed flow only depends on the coordinate y (1979), f, φ, h, π, r and θ depending only on y. Where α and β are the x and z components of the wavenumber vector \vec{k} , ω is the frequency and $f(y), \varphi(y), h(y), \pi(y), r(y), \theta(y)$ are the complex functions, or eigenfunctions, which gives the mode structure through the boundary layer. The normal modes are travelling waves in the x,z plane, and in the most general case, α, β and ω are all complex. If they are real, the wave is of the neutral stability and propagates in the x,z plane with constant amplitude and phase velocity $c = \omega / k$, where $k = (\alpha^2 + \beta^2)^{1/2}$ is the magnitude of \vec{k} . If any of α, β and ω are complex, the amplitude will change as the wave propagates.

When Eqs. (28) are substituted into Eqs. (19), (21)(23)(25), we obtain a system of non-parallel compressible flow equations:

Continuity Equation:

$$\begin{aligned} i[\alpha \overline{u} + \beta \overline{w} - \omega] r + \frac{d\overline{\rho}}{dy} \varphi + \frac{d\overline{v}}{dy} r + \overline{v} r' \\ + \overline{\rho} [\varphi' + i(\alpha f + \beta h)] = 0 \end{aligned} \quad (29)$$

The x-momentum Equation is:

$$\begin{aligned} \overline{\rho} \left[i[\alpha \overline{u} + \beta \overline{w} - \omega] f + \frac{d\overline{\mu}}{dy} \varphi + \overline{v} f' \right] + \overline{v} \frac{d\overline{\mu}}{dy} \\ = -i\alpha \pi + \overline{\mu} [f'' - (\alpha^2 + \beta^2) f] + \frac{d\overline{\mu}}{dT} \frac{dT}{dy} (f' + i\alpha \varphi) \\ + i\alpha (\overline{\lambda} + \overline{\mu}) [\varphi' + i(\alpha f + \beta h)] + \frac{d\overline{\mu}}{dT} \left(\theta \frac{d^2 \overline{u}}{dy^2} + \theta' \frac{d\overline{u}}{dy} \right) \\ + \frac{d^2 \overline{\mu}}{dT^2} \frac{d\overline{u}}{dy} \frac{dT}{dy} \theta + i\alpha \frac{d\overline{v}}{dy} \frac{d\overline{\lambda}}{dT} \theta \end{aligned} \quad (30)$$

The y-momentum Equation is:

$$\begin{aligned} \overline{\rho} \left[i[\alpha \overline{u} + \beta \overline{w} - \omega] \varphi + \frac{d\overline{v}}{dy} \varphi + \overline{v} \varphi' \right] + \overline{v} \frac{d\overline{v}}{dy} \\ = -\pi' + (\overline{\lambda} + \overline{\mu}) [\varphi'' + i(\alpha f' + \beta h')] \end{aligned}$$

$$\begin{aligned}
 & +\bar{\mu}\left[\bar{\varphi}' - (\alpha^2 + \beta^2)\bar{\varphi}\right] + \frac{d^2\bar{v}}{dy^2}\left[2\frac{d\bar{\mu}}{dT} + \frac{d\bar{\lambda}}{dT}\right]\theta \\
 & +\left[\bar{\varphi}' + i(\alpha f + \beta h)\right]\frac{d\bar{\lambda}}{dT}\frac{d\bar{T}}{dy} + \frac{d\bar{v}}{dy}\left[\frac{d\bar{\lambda}}{dT}\bar{\theta}' + \frac{d^2\bar{\lambda}}{dT^2}\frac{d\bar{T}}{dy}\bar{\theta}\right] \\
 & +2\bar{\varphi}'\frac{d\bar{\mu}}{dT}\frac{d\bar{T}}{dy} + \frac{d\bar{u}}{dy}\frac{d\bar{\mu}}{dT}i\alpha\theta + \frac{d\bar{w}}{dy}\frac{d\bar{\mu}}{dT}i\beta \\
 & +2\frac{d\bar{v}}{dy}\left[\frac{d\bar{\mu}}{dT}\bar{\theta}' + \frac{d^2\bar{\mu}}{dT^2}\frac{d\bar{T}}{dy}\bar{\theta}\right] \quad (31)
 \end{aligned}$$

The z-momentum equation is:

$$\begin{aligned}
 & \bar{\rho}\left[i\left[\alpha\bar{u} + \beta\bar{w} - \omega\right]h + \frac{d\bar{w}}{dy}\bar{\varphi} + \bar{v}h'\right] + \bar{v}\frac{d\bar{w}}{dy}r \\
 & = -i\beta\pi + (\bar{\lambda} + \bar{\mu})i\beta\left[\bar{\varphi}' + i(\alpha f + \beta h)\right] \\
 & + \frac{d\bar{\lambda}}{dT}\frac{d\bar{v}}{dy}i\beta\theta + \bar{\mu}\left[h' - (\alpha^2 + \beta^2)h\right] \\
 & + \left[(h' + i\beta\varphi)\right]\frac{d\bar{\mu}}{dT}\frac{d\bar{T}}{dy} + \frac{d\bar{\mu}}{dT}\left[\frac{d^2\bar{w}}{dy^2}\bar{\theta} + \frac{d\bar{w}}{dy}\bar{\theta}'\right] \\
 & + \frac{d^2\bar{\mu}}{dT^2}\frac{d\bar{T}}{dy}\frac{d\bar{w}}{dy}\bar{\theta} \quad (32)
 \end{aligned}$$

Energy Equation:

$$\begin{aligned}
 & c_v\bar{\rho}\left[i\left[\alpha\bar{u} + \beta\bar{w} - \omega\right]\theta + \frac{d\bar{T}}{dy}\bar{\varphi} + \bar{v}\theta'\right] + c_v\bar{v}\frac{d\bar{T}}{dy}r \\
 & = -\bar{p}\left[\bar{\varphi}' + i(\alpha f + \beta h)\right] - \frac{d\bar{v}}{dy}\pi + \left(\frac{d\bar{v}}{dy}\right)^2\frac{d\bar{\lambda}}{dT}\bar{\theta} \\
 & +2\bar{\lambda}\frac{d\bar{v}}{dy}\left[i(\alpha f + \beta h)\bar{\varphi}'\right] \\
 & +2\bar{\mu}\left[\frac{d\bar{u}}{dy}(f' + i\alpha\varphi) + 2\frac{d\bar{v}}{dy}\bar{\varphi}' + \frac{d\bar{w}}{dy}(h' + i\beta\varphi)\right] \\
 & + \frac{d^2\bar{T}}{dy^2}\frac{d\bar{\lambda}_c}{dT}\bar{\theta} + \left[\left(\frac{d\bar{u}}{dy}\right)^2 + 2\left(\frac{d\bar{v}}{dy}\right)^2 + \left(\frac{d\bar{w}}{dy}\right)^2\right]\frac{d\bar{\mu}}{dT}\bar{\theta} \\
 & +\bar{\lambda}_c\left[\bar{\theta}' - (\alpha^2 + \beta^2)\bar{\theta}\right] \\
 & + \frac{d\bar{T}}{dy}\left[\frac{d^2\bar{\lambda}_c}{dT^2}\frac{d\bar{T}}{dy}\bar{\theta} + 2\frac{d\bar{\lambda}_c}{dT}\bar{\theta}'\right] \quad (33)
 \end{aligned}$$

Equation of state :

$$\frac{\pi}{p} = \frac{r}{\rho} + \frac{\theta}{T} \quad (34)$$

2.5. Numerical Method of System Resolution:

Considering the boundary conditions derived from those associated with disturbances u', v', w', p', ρ' and T' , the differential system f, φ, h, π, r and θ corresponds to an eigenvalues problem, and the basic Eq. (28) of the compressible stability theory obtained are not yet in a form suitable for numerical computation. For this purpose we need a system of first-order equations (canonical system) $Z' = AZ$,

the lengthy equations for the matrix elements are listed in Appendix. The numerical resolution of this system is obtained using a numerical code adopted from the code developed at CERT/DERAT by Habiballah (1981) and Jelliti (1986). "This numerical resolution is undertaken from the free stream to the wall. For this shooting method, a fourth order Runge-Kutta technique has been used. The method of Gram-schmidt orthonormalization was also applied to stability equations and the Newton-Raphson procedure is satisfactory for obtaining the eigenvalues."

On the other hand, profiles $\bar{u}(y), \bar{v}(y), \bar{w}(y)$ and $\bar{T}(y)$ are provided by a numerical code developed at CERT/DERAT and solving the equations of the compressible boundary layer developing into self similar model (2008).

3. PARALLEL FLOW RESULTS

The present paper is mainly concerned with the spatial stability of the first mode for oblique waves nonparallel flow. However, some important parallel flow results are first given, to assess the validity of the present computations and the method of solution.

The present code was first used to compute stability characteristics for the compressible parallel flow, the results were in excellent agreement those obtained with the compressible formulation Mack (1984), Wazzan *et al.* (1984). The code was also used to compute the spatial stability of two-dimensional (2D) and three-dimensional (3D) disturbances at several Mach numbers for the transonic to supersonic compressible boundary layer.

For the transonic flow of adiabatic laminar flat plate boundary layer, two-dimensional waves, comparisons results are given in Figs.1, 2 for Mach number 0.9, where α_r , the real part of the wave, R is the Reynolds number, Me is the mach number and δ_i is the boundary layer displacement thickness.

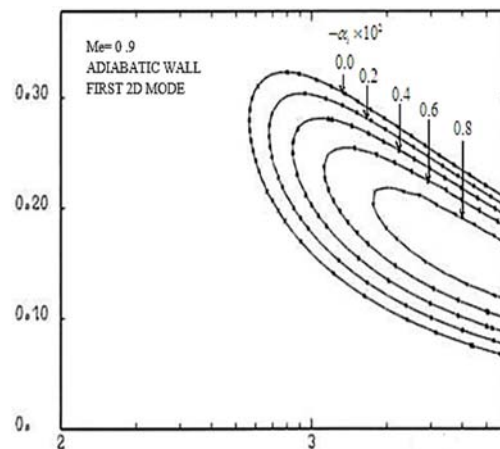


Fig. 1. Curves of constant spatial amplification rates; α_r as function of $\log_{10} R_{\delta_i}$: Computations of Jelliti (1986)

It seen the good agreement of the results and the similarity of the stability maps.

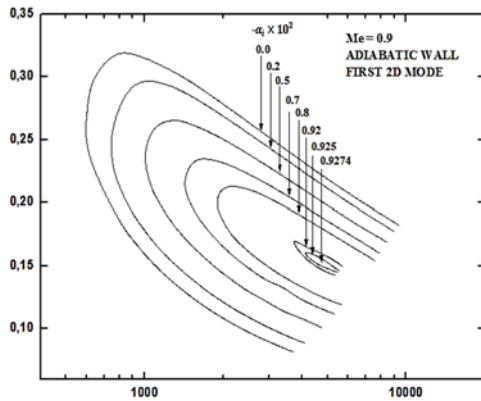


Fig. 2. Curves of constant spatial amplification rates; α_r as function of $\log_{10} R_{\delta_1}$: Present Computations.

Computations for the three-dimensional (3D) waves at $\psi = 35^\circ$ are given in Fig. 3, and showing that the maximum amplification rate is $\alpha_i = -0.9445 \cdot 10^{-2}$ and has a critical Reynolds number $R_{\delta_1} = 662,6$. However, as shown in Fig. 1 for the two dimensional (2D) waves, the the maximum amplification rate is $\alpha_i = -0.9274 \cdot 10^{-2}$ and has a critical Reynolds number $R_{\delta_1} = 589.5$, consequently these values increase with the 3D waves.

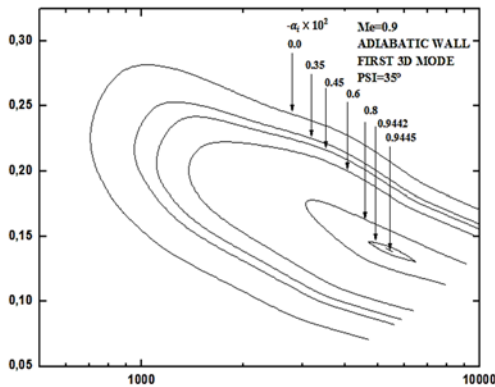


Fig. 3. Curves of constant spatial amplification rates α_r as function of $\log_{10} R_{\delta_1}$: Present Computations.

Results for $Me=1.1$ ($\psi = 40^\circ$) are shown in Fig. 4 giving a critical Reynolds number $R_{\delta_1} = 733,4$ for the 3D waves.

Similarly, results, Figs. 3, 5, for the supersonic flow are computed for $Me = 2.2$ ($\psi = 0^\circ$ and $\psi = 60^\circ$), whereas the corresponding values decreases with the 3D disturbances, the critical Reynolds number $R_{\delta_1} = 901$ for the oblique mode is smaller than the corresponding value of 1065 for the 2D mode.

We can also see by comparing the results of two-dimensional disturbances at $Me = 0.9$ and 2.2 that the critical Reynolds number increase with increasing Mach number whereas the maximum amplification rate at low Reynolds number decreases with increasing Mach number. These results are in good agreement with those obtained by Wazzan *et al.* (1984) for $Me = 1.6$ and $Me = 2.2$.

The 2D compressible stability calculations (1947, 1965) showed a precipitous decrease in viscous instability with increasing Mach number.

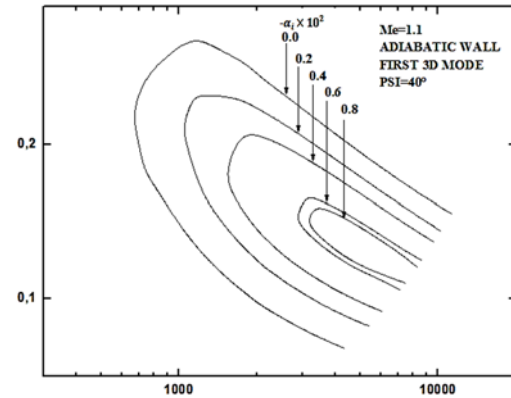


Fig. 4. Curves of constant spatial amplification rates α_r as function of Reynolds number R_{δ_1} : present computations.

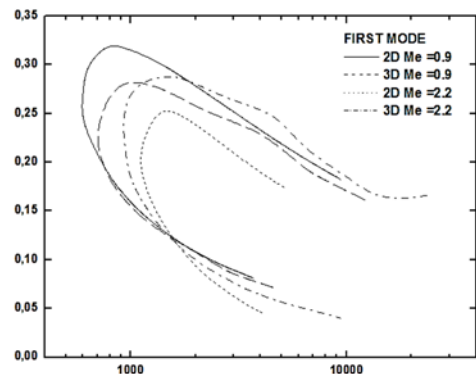


Fig. 5. Computations of neutral stability curve (α_r as function of $\log_{10} R_{\delta_1}$).

The 3D waves for the first mode is more unstable than the 2D waves only when the Mach number becomes higher than 1. The reason why we are interested particularly in the Mach number 0.9 by comparing it with higher Mach numbers. Indeed, as shown in Fig.5 presenting the neutral curve (on the wavenumber-Reynolds-number diagram) for $Me = 0.9$ and 2.2 at respectively wave angle $\psi = 35^\circ$ and 60° the wave instability appears clearly at $Mach > 1$.

Consequently, the purpose of presenting the diagrams of maximum amplification rates for the two corresponding Mach numbers Fig. 6 is to show the phenomenon of viscosity instability which its mechanism was first demonstrated by Prandtl (1921), where the maximum of amplification rates increases with decreasing Reynolds number (of a

given frequency).

The code was also checked against the neutral stability computations by Mack (1965) at Mach 2.2 and measurements of Laufer and Vrebalovich (1970) given in Fig. 8; results were made for both two-dimensional ($\psi = 0^\circ$) and oblique disturbances ($\psi = 45^\circ, 60^\circ$).

Comparing also with the results given by Wazzan *et al.* (1984), it seen the good agreement between computations and measurements.

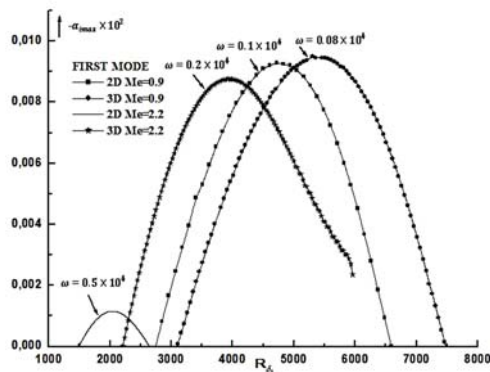


Fig. 6. Maximum amplification rates as function of Reynolds number at given frequency.

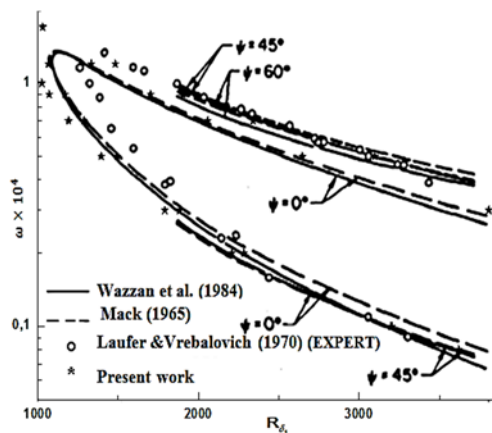


Fig. 7. Neutral stability curve at Mach 2.2 for adiabatic flat plate.

Figure 8 gives, the neutral curve for the first mode of 2D and oblique waves ($\psi = 60^\circ$) at $Me = 2.2$, showing that the oblique wave is more unstable than the two-dimensional disturbance. However, by comparing results with those of the transonic flow $Me = 0.9$, it seen that the 2D waves is more unstable than the oblique waves.

We see that given Mach number, there is a critical Reynolds number below which all disturbances are damped, whatever of their frequency.

In the present computations, maps of the spatial amplification rates on the frequency-Reynolds number diagram for Mach numbers $Me = 1.6$ and $Me = 2.2$, are given in Figs. 9 and 11.

Results of the two Mach numbers appear similar to

stability maps given by Wazzan *et al.* (1984), Figs.10 and 12, showing that the maximum amplification rate at low Reynolds number decreases with increasing Mach number.

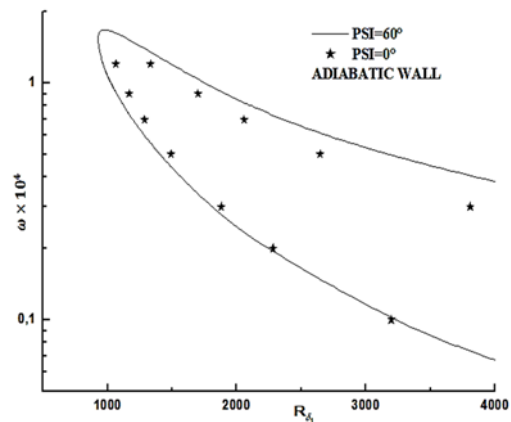


Fig. 8. Neutral stability curve at Mach 2.2 for adiabatic flat plate: Present Computations.

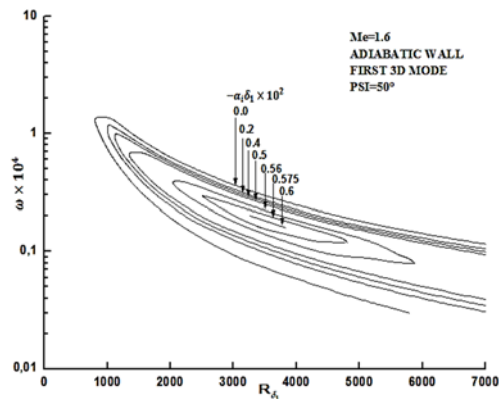


Fig. 9. Curves of constant spatial amplification rates: present computations.

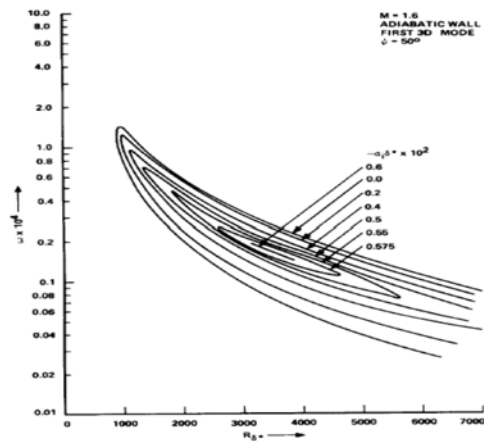


Fig. 10. Curves of constant spatial amplification rates: computations of Wazzan *et al.* (1984).

However, according to Mack (1969) and Wazzan *et al.* (1984), the most unstable wave angle varies, particularly at low Mach numbers, with the Reynolds number; this wave angle increases rapidly with Mach number ($Me = 1.6$ to 2.2). They suggest, that the most dangerous wave angle for each Mach number

(computations for the spatial amplification rate are made as a function of frequency for given values of the wave angle ψ and at a fixed Reynolds number), are respectively $\psi = 60^\circ$ and 50° at Mach $Me = 2.2$ and 1.6

Comparing the results given in Figs.9 and 10, disturbances at $Me = 1.6$ ($\psi = 50^\circ$) show that the maximum viscous amplification rate ($-\alpha_i \delta_i \times 10^3$) is in order to 0.6, a highest-amplified frequency under than $2 \cdot 10^{-4}$, and a critical Reynolds number $R_{\delta_i} = 775$.

Similarly, results for $Me = 2.2$ given in Figs.11 and 12 is in order to 0.77, a highest amplified frequency under than $2 \cdot 10^{-4}$, and a critical Reynolds number $R_{\delta_i} = 901$.

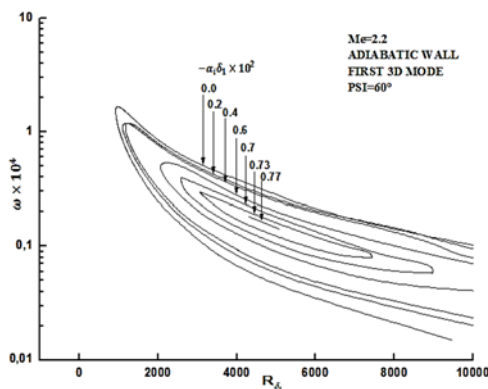


Fig. 11. Curves of constant spatial amplification rates: Present Computations.

When Mach number increases the height of generalized inflection point increases: simultaneously, the range of unstable wave numbers at finite Reynolds is expanding, and the inflectional instability is seen at low Reynolds number (1986).

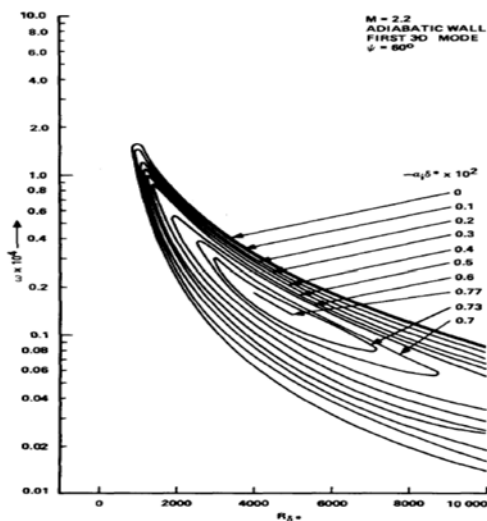


Fig. 12. Curves of constant spatial amplification rates: computations of Wazzan *et al.* (1984).

According to the comparing results, we deduce the

good agreement with the general computation given by Wazzan *et al.* (1984) and Mack (1984).

It should be noted, comparing with the 2D results, (according to Wazzan *et al.* (1984) and Mack (1984) that the most unstable first mode is always that the oblique waves.

Effect of the wave angle ψ

Figure 13 shows the evolution of the maximum value of local amplification rate as a function of wave number ψ at fixed Reynolds number in the range Mach 0.9, 1.1, 1.3, 1.6 and 2.2. At $Me = 0.9$, $\alpha_{i,max}$ remains constant in a wide range of wave number. At a higher Mach numbers a maximum appears for a $\psi \neq 0^\circ$ noted $\alpha_{max} \cdot \alpha_{max}$ depends on the Reynolds number at fixed Mach number, but this dependence is weak.

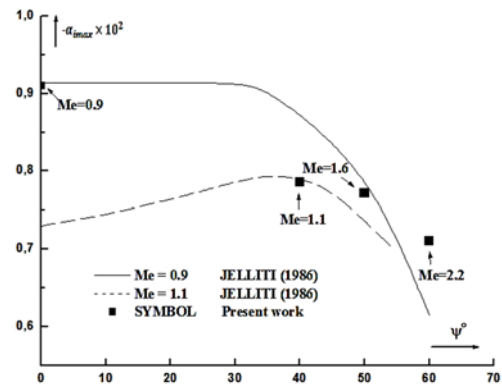


Fig. 13. Coefficients of maximal amplification rate as function of the wave angle ψ .

4. NONPARALLEL FLOW RESULTS

The present code is used to compute the spatial stability of bidimensional and three-dimensional disturbances nonparallel flow.

Figures 14, 15 give, for the first mode of 2D and oblique waves, maps of the spatial amplification rates on the wavenumber-Reynolds number diagram for Mach 0.9 and 1.1

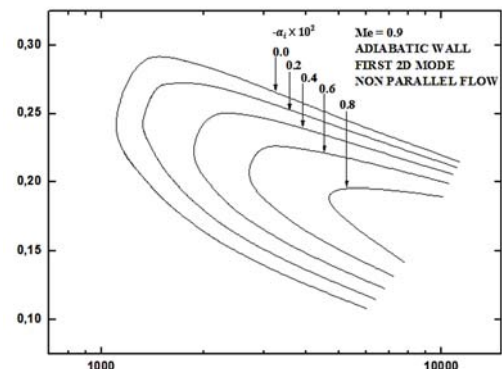


Fig. 14. Curves of constant spatial amplification rates nonparallel flow (α_r as function of $\log_{10} R_{\delta_i}$).

The neutral curves for 2D at $Me = 0.9$ and oblique waves ($\psi = 40^\circ$) at $Me = 1.1$ are shown in Figs. 16 and 17.

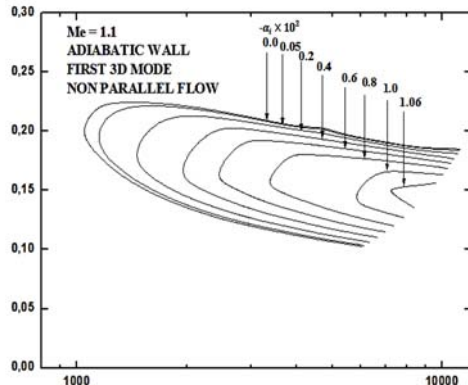


Fig. 15. Curves of constant spatial amplification rates nonparallel flow (α_r as function of $\log_{10} R_{\delta_1}$).

It covers the wavenumber $\alpha_r = 0.05$ to 0.29 and has a critical Reynolds number $R_{\delta_1} = 1057$ for $Me = 0.9$,

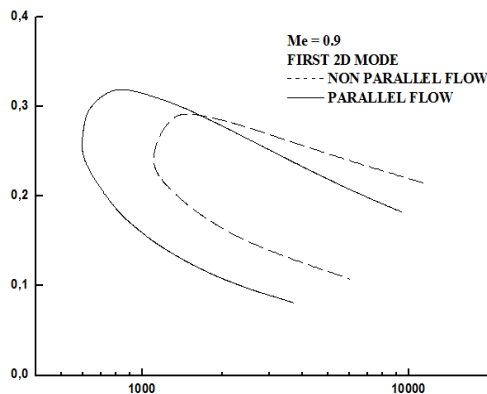


Fig. 16. Comparison Curves of constant spatial amplification rates parallel and nonparallel flow (α_r as function of $\log_{10} R_{\delta_1}$).

These values compare with $\alpha_r = 0.09$ to 0.22 and critical $R_{\delta_1} = 1030$ for $Me = 1.1$ ($\psi = 40^\circ$).

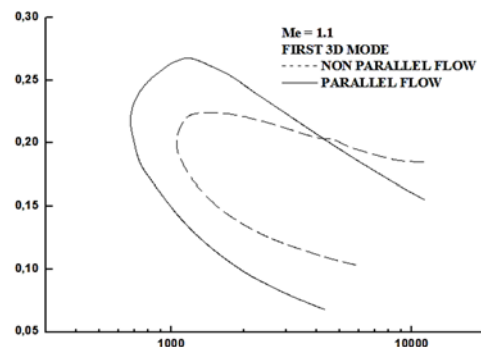


Fig. 17. Comparison Curves of constant spatial amplification rates parallel and nonparallel flow (α_r as function of $\log_{10} R_{\delta_1}$).

It seen that the critical Reynolds number decreases with increasing Mach number which differ from the parallel flow as shown previously.

Figure 18 compares also the maximum amplification rate curves for the parallel 2D and oblique waves with the maximum amplification rate curves for the nonparallel 2D and oblique waves.

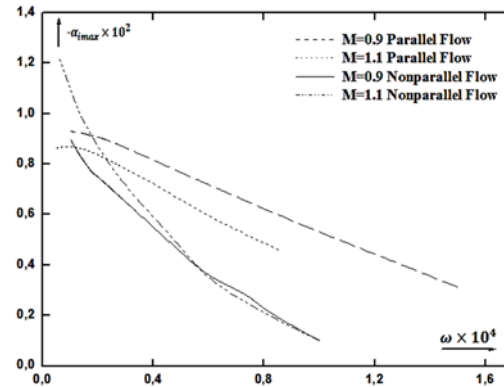


Fig. 18. Comparison Curves of maximal amplification rate parallel and nonparallel flow.

It illustrates that the bidimensional parallel flow is more unstable than the nonparallel flow for the smaller even the higher frequency. However, as shown, to the figure for the oblique disturbances, it seen that the parallel flow is more unstable than the nonparallel flow at a precise frequency value.

The present results show the importance of the wave angle ψ for the parallel and nonparallel flow to the 2D and oblique disturbances.

5. CONCLUSIONS

The present work treated for the laminar boundary layer on a compressible fluid which linearized spatial stability of adiabatic flat plate flow to the first mode of the bi and three-dimensional disturbances are computed numerically over the entire Reynolds number and Mach number range of interest $Me = 0.9$ ($\psi = 0^\circ, 35^\circ$) to 2.2 for the parallel flow and $Me = 0.9$ to 1.1 for the nonparallel flow which constitute the original contribution of this paper.

Stability maps, in the form of familiar curves of constant spatial amplification rate are presented. The general computations results presented for the parallel flow are in good agreement with those obtained by Jelliti, Mack and Wazzan, Taghavi and Keltner showing essentially that the most unstable first mode is the first mode for oblique waves which leads us to conclude the validation of the compressible stability calculation code elaborated by present calculations.

The present computations, concerned the nonparallel flow give important results by comparing with the parallel flow, both for the 2D and the oblique waves; illustrating that the parallel flow is more unstable than the nonparallel flow for the bidimensional

waves (at all frequencies), however, for the oblique disturbances the parallel flow is more unstable than the non parallel flow only at a precise value of frequency. These results even for the parallel flow show the importance of the wave angle ψ .

The stability diagrams presented in this paper give important results concerned the Reynolds number of nonparallel flow which differ from the parallel flow, showing that the critical Reynolds number decreases with increasing Mach number.

IN MEMORY

On the occasion of this article, the authors honor the memory of their late friend Miloud Jelliti who initiated this research

REFERENCES

Arnal, D. and M. Jelliti (1986). Colloquium on the Turbulent Compressible Flows, Poitiers.

Brooker, A. M. H., J. C. Patterson and S.W. Armfield (1997). Non parallel linear stability analysis of the vertical boundary layer in a differentially heated cavity. *Journal of Fluid Mechanics* 352, 265-281.

Brown, W. B. (1962). *Norair Report NOR-62-15*. Northrop Corporation, Hawthorne, California.

Brown, W. B. (1961). In *Boundary Layer and Flow Control*, edited by G.V. Lachmann, 2, 1033.

Chiquette, C. (2007). *Nonparallel theory*. Hydrodynamic Stability, literature project.

Chang, C. L., M. R. Malik, G. Erlebacher and M. Yousuff Hussaini (1993). Linear and nonlinear PSE for compressible boundary layers. *NASA Report No.93-70*.

Fasel, H., U. Rist and U. Konzelmann (1990). Numerical investigation of the three dimensional development in boundary layer transition. *AIAA J.* 28(1), 29-37.

Gaster, M. (1965). On the generation of spatially growing waves in a boundary layer. *J. Fluid Mech.* 22, 433-441.

Habiballah, M. (1981). *Analysis of The Instability of laminar boundary layers and Prediction of Transition of Laminar to Turbulent Regime*, Ph. D. Thesis, ENSAE.

Jelliti, M. (1986). *Transition of Laminar to Turbulent Regime: Effects of Tridimensionality and Compressibility*, Ph. D. Thesis, ONERA.

Krimmelbein, N. and R. Radespiel (2008). Transition prediction for three dimensional flows using parallel computations. *Computers and Fluids* 38,121-136.

Laufer, J. and T. Vrebalovich (1970). *J. Fluid Mech.* 9, 257.

Lees, L. (1947). NACA Report No.876.

Lees, L. and C. C. Lin (1946). investigation of the

stability of the laminar boundary layer in a compressible fluid. *NACA Tech.note No.1115*.

Lin, C.C. (1945) On the stability of Two-Dimensional Parallel Flows, Part I, II, III, *Quart. Appl. Math* 3, 117-142.

Lin, C.C. (1945) On the stability of Two-Dimensional Parallel Flows, Part I, II, III, *Quart. Appl. Math* 3, 218-234.

Lin, C.C. (1945) On the stability of Two-Dimensional Parallel Flows, Part I, II, III, *Quart. Appl. Math* 3, 277-301.

Mack, L. M. (1965). AGARDograph 97,483.

Mack, L. M. (1969). Jet Propulsion Lab, Pasadena, California, Report, 900-277, Rev. A.

Mack, L. M. (1984). Boundary layer linear stability theory, special course on stability and transition of laminar flow. *AGARD Report No.709*.

Mack, L. M. (1965). *Methods in Computational Physics*, edited by B.Alder Vol.4, 247.

Mérida, Y. (2008). *Laminar Instability of Tridimensionel Compressible Flow : Application to Stability diagrams*, Master, Fst.

Monin, A. S. and A. M. Yaglom (1979). *Statistical Fluid Mechanics of Turbulence*. MIT Press.

Prandtl, L. (1921) *ZAMM* 1,431.

Saric, W. S. and A. H. Nayfeh (1975). Nonparallel stability of boundary-layer flows. *Phys. Fluids* 18, 945-950.

Sousa, J. M. M. and L. M. G. Silva (2004). Transition prediction in infinite swept wings using Navier-stokes computations and linear stability theory. *Computers and Structures* 82, 1551-1560.

Wazzan, A. R., H. Taghavi and G. Keltner (1984). The effect of mach number on the spatial stability of adiabatic flat plate flow to oblique disturbances. *Phys. Fluid* 27(2), 331-341.

APPENDIX

The dependent variables of the system $Z'=AZ$ are defined by:

$$Z_1 = f, Z_2 = f', Z_3 = \varphi, Z_4 = \varphi', Z_5 = h, Z_6 = h', Z_7 = \pi, Z_8 = \theta, Z_9 = \theta'$$

Where: $Z'_1 = Z_2, Z'_3 = Z_4, Z'_5 = Z_6, Z'_8 = Z_9$

The system of equations (28) to (34) provides the linear forms giving the expressions for the matrix elements A:

$$Z'_7 = -i \frac{\bar{p}}{v} \alpha Z_1 - \frac{1}{v} \frac{\bar{p}}{v} \frac{d\bar{p}}{dy} Z_3 - \frac{\bar{p}}{v} Z_4 - i \frac{\bar{p}}{v} \beta Z_5$$

$$- \left[\frac{i}{v} (\alpha \bar{u} + \beta \bar{w} - \omega) + \frac{1}{v} \frac{d\bar{v}}{dy} - \frac{1}{T} \frac{d\bar{T}}{dy} \right] Z_7$$

$$\begin{aligned}
 & + \left[\frac{i}{v} (\alpha \bar{u} + \beta \bar{w} - \omega) + \frac{1}{v} \frac{d\bar{v}}{dy} + \frac{1}{\rho} \frac{d\bar{\rho}}{dy} - \frac{1}{T} \frac{d\bar{T}}{dy} \right] \frac{\bar{p}}{T} Z_8 \\
 & + \frac{\bar{p}}{T} Z_9 \\
 Z_2 = & \left[i \frac{\bar{\rho}}{\mu} (\alpha \bar{u} + \beta \bar{w} - \omega) + (\alpha^2 + \beta^2) + \alpha^2 \left(\frac{\bar{\lambda} + \bar{\mu}}{\mu} \right) \right] Z_1 \\
 & + \left[\frac{\bar{\rho} \bar{v}}{\mu} - \frac{1}{\mu} \frac{d\bar{\mu}}{dy} \frac{d\bar{T}}{dy} \right] Z_2 + \left[\frac{\bar{\rho} d\bar{u}}{\mu dy} - i\alpha \frac{1}{\mu} \frac{d\bar{\mu}}{dT} \frac{d\bar{T}}{dy} \right] Z_3 \\
 & - \left[i\alpha \left(\frac{\bar{\lambda} + \bar{\mu}}{\mu} \right) \right] Z_4 + \left[\alpha\beta \left(\frac{\bar{\lambda} + \bar{\mu}}{\mu} \right) \right] Z_5 \\
 & + \left[i \frac{\alpha}{\mu} + \frac{\bar{\rho} \bar{v}}{p \mu} \frac{d\bar{u}}{dy} \right] Z_7 \\
 & - \left[\frac{\bar{\rho} \bar{v} d\bar{u}}{T \mu dy} + \frac{1}{\mu} \frac{d\bar{\mu}}{dT} \frac{d^2 \bar{u}}{dy^2} + \frac{1}{\mu} \frac{d^2 \bar{\mu}}{dT^2} \frac{d\bar{u}}{dy} + i \frac{\alpha}{\mu} \frac{d\bar{v}}{dy} \frac{d\bar{\lambda}}{dT} \right] Z_8 \\
 & - \left[\frac{1}{\mu} \frac{d\bar{\mu}}{dT} \frac{d\bar{u}}{dy} \right] Z_9 \\
 Z_4 = & \left[-\frac{i\alpha}{(\bar{\lambda} + 2\bar{\mu})} \left(\frac{\bar{p}}{v} + \frac{d\bar{\lambda}}{dT} \frac{d\bar{T}}{dy} \right) \right] Z_1 \\
 & - \left[\frac{(\bar{\lambda} + \bar{\mu})}{(\bar{\lambda} + 2\bar{\mu})} i\alpha \right] Z_2 \\
 & + \left[\frac{1}{(\bar{\lambda} + 2\bar{\mu})} \left(i\bar{\rho} (\alpha \bar{u} + \beta \bar{w} - \omega) + \bar{\rho} \frac{d\bar{v}}{dy} + \right) \right] Z_3 \\
 & + \left[\frac{1}{(\bar{\lambda} + 2\bar{\mu})} \left(\bar{\rho} \bar{v} - \frac{d\bar{\lambda}}{dT} \frac{d\bar{T}}{dy} - 2 \frac{d\bar{\mu}}{dT} \frac{d\bar{T}}{dy} - \frac{\bar{p}}{v} \right) \right] Z_4 \\
 & - \left[\frac{i\beta}{(\bar{\lambda} + 2\bar{\mu})} \left(\frac{d\bar{\lambda}}{dT} \frac{d\bar{T}}{dy} + \frac{\bar{p}}{v} \right) \right] Z_5 - \left[\frac{(\bar{\lambda} + \bar{\mu})}{(\bar{\lambda} + 2\bar{\mu})} i\beta \right] Z_6 \\
 & + \left[\frac{1}{(\bar{\lambda} + 2\bar{\mu})} \left(\frac{\bar{v} d\bar{v}}{v} \frac{\bar{\rho}}{p} - \frac{i}{v} (\alpha \bar{u} + \beta \bar{w} - \omega) \right) \right] Z_7 \\
 & + \left[\frac{1}{(\bar{\lambda} + 2\bar{\mu})} \left(-\frac{1}{v} \frac{d\bar{v}}{dy} + \frac{1}{T} \frac{d\bar{T}}{dy} \right) \right] Z_9 \\
 & - \left[\frac{1}{(\bar{\lambda} + 2\bar{\mu})} \left(\frac{\bar{v} d\bar{v}}{v} \frac{\bar{\rho}}{T} + \frac{d^2 \bar{v}}{dy^2} \left(\frac{d\bar{\lambda}}{dT} + 2 \frac{d\bar{\mu}}{dT} \right) + \frac{d\bar{v}}{dy} \frac{d^2 \bar{\lambda}}{dT^2} \frac{d\bar{T}}{dy} \right) \right. \\
 & \left. + i \left(\alpha \frac{d\bar{u}}{dy} \frac{d\bar{\mu}}{dT} + \beta \frac{d\bar{w}}{dy} \frac{d\bar{\mu}}{dT} \right) + 2 \frac{d\bar{v}}{dy} \frac{d^2 \bar{\mu}}{dT^2} \frac{d\bar{T}}{dy} \right] Z_8 \\
 & - \left[\frac{i}{v} (\alpha \bar{u} + \beta \bar{w} - \omega) + \frac{1}{v} \frac{d\bar{v}}{dy} + \frac{1}{\rho} \frac{d\bar{\rho}}{dy} - \frac{1}{T} \frac{d\bar{T}}{dy} \right] \frac{\bar{p}}{T}
 \end{aligned}$$

$$\begin{aligned}
 & - \left[\frac{1}{(\bar{\lambda} + 2\bar{\mu})} \left(\frac{\bar{p}}{T} - \frac{d\bar{v}}{dy} \left(\frac{d\bar{\lambda}}{dT} + 2 \frac{d\bar{\mu}}{dT} \right) \right) \right] Z_9 \\
 Z_6 = & \left[\frac{(\bar{\lambda} + \bar{\mu})}{\mu} \alpha\beta \right] Z_1 + \left[\frac{1}{\mu} \left(\bar{\rho} \frac{d\bar{w}}{dy} - \frac{d\bar{\mu}}{dT} \frac{d\bar{T}}{dy} i\beta \right) \right] Z_3 \\
 & - \left[\frac{(\bar{\lambda} + \bar{\mu})}{\mu} i\beta \right] Z_4 \\
 & + \left[\frac{1}{\mu} \left(i\bar{\rho} (\alpha \bar{u} + \beta \bar{w} - \omega) + \beta^2 (\bar{\lambda} + \bar{\mu}) + \bar{\mu} (\alpha^2 + \beta^2) \right) \right] Z_5 \\
 & + \left[\frac{1}{\mu} \left(\bar{\rho} \bar{v} - \frac{d\bar{\mu}}{dT} \frac{d\bar{T}}{dy} \right) \right] Z_6 + \left[\frac{1}{\mu} \left(\bar{v} \frac{d\bar{w}}{dy} \frac{\bar{\rho}}{p} + i\beta \right) \right] Z_7 \\
 & + \left[\frac{1}{\mu} \left(-\bar{v} \frac{d\bar{w}}{dy} \frac{\bar{\rho}}{T} - \frac{d\bar{\mu}}{dT} \frac{d^2 \bar{w}}{dy^2} - \frac{d^2 \bar{\mu}}{dT^2} \frac{d\bar{w}}{dy} \frac{d\bar{T}}{dy} - \frac{d\bar{\lambda}}{dT} \frac{d\bar{v}}{dy} i\beta \right) \right] Z_8 \\
 & - \left[\frac{1}{\mu} \frac{d\bar{\mu}}{dT} \frac{d\bar{w}}{dy} \right] Z_9 \\
 Z_9 = & \left[\frac{1}{\lambda_c} \left(i\alpha \bar{p} - 2i\alpha \bar{\lambda} \frac{d\bar{v}}{dy} \right) \right] Z_1 - \left[2 \frac{\bar{\mu}}{\lambda_c} \frac{d\bar{u}}{dy} \right] Z_2 \\
 & + \left[\frac{1}{\lambda_c} \left(c_v \bar{\rho} \frac{d\bar{T}}{dy} - 2i\alpha \bar{\mu} \frac{d\bar{u}}{dy} - 2i\beta \bar{\mu} \frac{d\bar{w}}{dy} \right) \right] Z_3 \\
 & + \left[\frac{1}{\lambda_c} \left(\bar{p} - 2\bar{\lambda} \frac{d\bar{v}}{dy} - 4\bar{\mu} \frac{d\bar{v}}{dy} \right) \right] Z_4 \\
 & + \left[\frac{1}{\lambda_c} \left(i\beta \bar{p} - 2i\beta \bar{\lambda} \frac{d\bar{v}}{dy} \right) \right] Z_5 - \left[2 \frac{\bar{\mu}}{\lambda_c} \frac{d\bar{w}}{dy} \right] Z_6 \\
 & + \left[\frac{1}{\lambda_c} \left(c_v \bar{v} \frac{\bar{\rho}}{p} \frac{d\bar{T}}{dy} + \frac{d\bar{v}}{dy} \right) \right] Z_7 \\
 & + \left[\frac{1}{\lambda_c} \left(i c_v \bar{\rho} (\alpha \bar{u} + \beta \bar{w} - \omega) - c_v \bar{v} \frac{\bar{\rho}}{T} \frac{d\bar{T}}{dy} - \left(\frac{d\bar{v}}{dy} \right)^2 \frac{d\bar{\lambda}}{dT} \right) \right. \\
 & \left. - \frac{d\bar{\mu}}{dT} \left(\left(\frac{d\bar{u}}{dy} \right)^2 + 2 \left(\frac{d\bar{v}}{dy} \right)^2 + \left(\frac{d\bar{w}}{dy} \right)^2 \right) \right. \\
 & \left. - \bar{\lambda}_c (\alpha^2 + \beta^2) - \frac{d^2 \bar{T}}{dy^2} \frac{d\bar{\lambda}_c}{dT} - \frac{d^2 \bar{\lambda}_c}{dT^2} \left(\frac{d\bar{T}}{dy} \right)^2 \right] Z_8
 \end{aligned}$$